

Tuning-Free Structured Sparse PCA via Deep Unfolding Networks

Long Chen and Xianchao Xiu

School of Mechatronic Engineering and Automation, Shanghai University, Shanghai 200444, China
E-mail: 150538cli@shu.edu.cn, xcxiu@shu.edu.cn

Abstract: Sparse principal component analysis (PCA) is a well-established dimensionality reduction technique that is often used for unsupervised feature selection (UFS). However, determining the regularization parameters is rather challenging, and conventional approaches, including grid search and Bayesian optimization, not only bring great computational costs but also exhibit high sensitivity. To address these limitations, we first establish a structured sparse PCA formulation by integrating ℓ_1 -norm and $\ell_{2,1}$ -norm to capture the local and global structures, respectively. Building upon the off-the-shelf alternating direction method of multipliers (ADMM) optimization framework, we then design an interpretable deep unfolding network that translates iterative optimization steps into trainable neural architectures. This innovation enables automatic learning of the regularization parameters, effectively bypassing the empirical tuning requirements of conventional methods. Numerical experiments on benchmark datasets validate the advantages of our proposed method over the existing state-of-the-art methods. Our code will be accessible at <https://github.com/xianchaoxiu/SPCA-Net>.

Key Words: Deep unfolding networks, principal component analysis (PCA), structured sparse, tuning-free, unsupervised feature selection (UFS)

1 Introduction

Unsupervised feature selection (UFS) has emerged as a critical technique in high-dimensional data analysis, particularly for image and signal processing applications where class labels are often unavailable; see [1–3] for a recent survey. Among various approaches, sparse principal component analysis (PCA) [4] has become a prominent UFS tool, demonstrating remarkable success across diverse domains ranging from image processing [5, 6], fault diagnosis [7, 8] to natural language processing [9, 10].

Let $A \in \mathbb{R}^{d \times n}$ denote the data matrix. Mathematically, the classical PCA can be formulated as

$$\begin{aligned} \min_X \quad & \frac{1}{2} \|A - XX^\top A\|_F^2 \\ \text{s.t.} \quad & X^\top X = I, \end{aligned} \quad (1)$$

where $X \in \mathbb{R}^{d \times m}$ is the projection matrix and $I \in \mathbb{R}^{m \times m}$ is the identity matrix. However, it suffers from limited feature interpretability. To address this issue, sparse PCA was proposed in [11] by defining

$$\begin{aligned} \min_X \quad & \frac{1}{2} \|A - XX^\top A\|_F^2 + \lambda \|X\|_1 \\ \text{s.t.} \quad & X^\top X = I, \end{aligned} \quad (2)$$

where $\|X\|_1$ is the ℓ_1 -norm, defined as the sum of absolute values of all elements, and λ is the regularization parameter. By enforcing the ℓ_1 -norm and adjusting λ , sparse PCA can obtain a sparse projection matrix, thereby enhancing the interpretability and alleviating the interference of noise. However, two fundamental challenges remain.

On the one hand, the ℓ_1 -norm in sparse PCA only exploits element-wise sparsity, which often lead to biased solutions [12]. This limitation becomes particularly apparent in applications where features naturally exhibit group-wise sparsity,

which cannot be characterized by ℓ_1 -norm but could be captured by $\ell_{2,1}$ -norm (defined as the sum of ℓ_2 -norm of each row) [13, 14]. Current methodologies usually consider these sparsity-inducing norms separately or apply them to different variables, while it remains an open question whether the integration of ℓ_1 -norm and $\ell_{2,1}$ -norm with PCA could yield superior performance in the field of UFS.

On the other hand, traditional parameter selection strategies (e.g., grid search, Bayesian optimization) face significant scalability limitations in high-dimensional settings [15–17]. The emerging paradigm of deep unfolding networks [18] offers a promising alternative by embedding optimization mechanics into neural architectures through algorithmic unfolding, i.e., transforming the iterative algorithm steps into network layers [19–21]. This approach combines mathematical interpretability with neural network efficiency, achieving excellent performance in many fields such as communications [22], compressive sensing [23], and infrared small target detection [24]. Notably, deep unfolding networks typically require fewer trainable parameters than conventional deep architectures, which substantially reduces the computational complexity and training costs [25, 26]. Despite these advancements, the application of deep unfolding networks to PCA-based UFS remains absent from the literature.

Inspired by sparse group Lasso [27], we propose the following structured sparse PCA formulation

$$\begin{aligned} \min_X \quad & \frac{1}{2} \|A - XX^\top A\|_F^2 + \lambda \|X\|_{2,1} + \mu \|X\|_1 \\ \text{s.t.} \quad & X^\top X = I, \end{aligned} \quad (3)$$

where $\lambda, \mu > 0$ are the regularization parameters, ℓ_1 -norm and $\ell_{2,1}$ -norm are introduced to capture local and global structures, respectively, thus play a complementary role. Departing from conventional first-order optimization algorithms with manual parameter tuning, we develop an intelligent solution through deep unfolding networks that automatically learns optimal parameter configurations. For convenience, we call this method SPCA-Net.

This work was supported by the National Natural Science Foundation of China under Grant 12371306. (Corresponding author: Xianchao Xiu.)

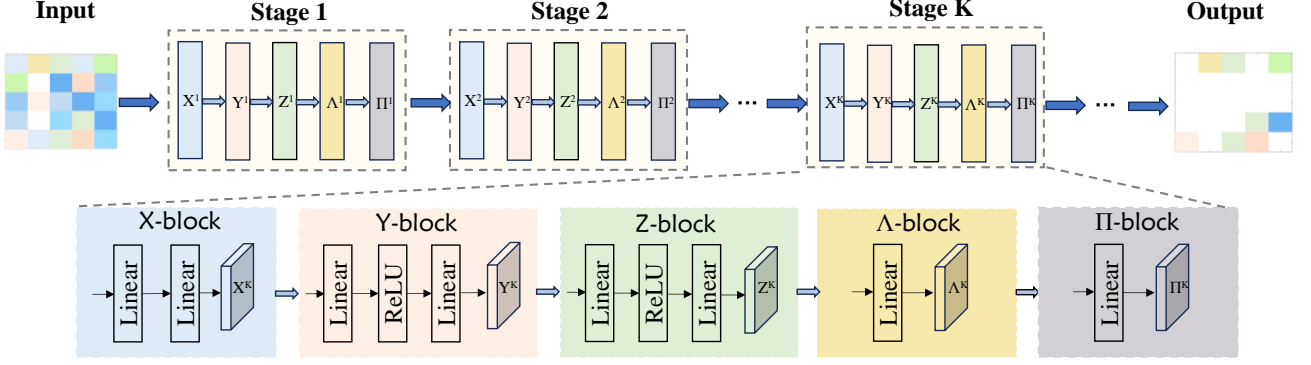


Fig. 1: Overview of the proposed SPCA-Net.

The contributions of this paper are twofold.

- A novel structured sparse PCA framework integrating ℓ_1 -norm and $\ell_{2,1}$ -norm is proposed to enhance UFS.
- A pioneering deep unfolding networks-based algorithm is developed that combines mathematical priors with data-driven efficiency; see Fig. 1.

2 Methodology

This section describes how to leverage deep unfolding networks to develop a tuning-free algorithm for problem (3). Technically, we unfold each step of the alternating direction method of multipliers (ADMM) [28] into a layer in neural networks, thus transforming parameters into learnable ones.

We first introduce auxiliary variables $Y, Z \in \mathbb{R}^{d \times m}$ and reformulate problem (3) as

$$\begin{aligned} \min_{X, Y, Z} \quad & \frac{1}{2} \|A - XX^\top A\|_F^2 + \lambda \|Y\|_{2,1} + \mu \|Z\|_1 \\ \text{s.t.} \quad & X^\top X = I, X = Y, X = Z. \end{aligned} \quad (4)$$

The corresponding augmented Lagrangian function is

$$\begin{aligned} \mathcal{L}(X, Y, Z, \Lambda, \Pi) &= \frac{1}{2} \|A - XX^\top A\|_F^2 + \lambda \|Y\|_{2,1} + \mu \|Z\|_1 \\ &+ \langle \Lambda, X - Y \rangle + \frac{\alpha}{2} \|X - Y\|_F^2 \\ &+ \langle \Pi, X - Z \rangle + \frac{\beta}{2} \|X - Z\|_F^2, \end{aligned} \quad (5)$$

where Λ and Π are the Lagrange multipliers, and $\alpha, \beta > 0$ are penalty parameters. Now we can update one variable while fixing others, which is the well-known ADMM.

2.1 Update X^{k+1}

It can be equivalently transformed into

$$\begin{aligned} \min_X \quad & \frac{1}{2} \|A - XX^\top A\|_F^2 + \frac{\alpha}{2} \|X - Y^k + \Lambda^k/\alpha\|_F^2 \\ & + \frac{\beta}{2} \|X - Z^k + \Pi^k/\beta\|_F^2 \\ \text{s.t.} \quad & X^\top X = I, \end{aligned} \quad (6)$$

which does not have a closed-form solution. Denote the objective function of (6) as $f(X)$. Using linearization with

approximation parameter $\eta > 0$, we derive

$$\begin{aligned} \min_X \quad & f(X^k) + \langle \nabla f(X^k), X - X^k \rangle \\ & + \frac{1}{2\eta} \|X - X^k\|_F^2 \\ \text{s.t.} \quad & X^\top X = I, \end{aligned} \quad (7)$$

which can be simplified to

$$\begin{aligned} \min_X \quad & (AA^\top X^k + (\alpha(X^k - Y^k + \Lambda^k/\alpha) \\ & + \beta(X^k - Z^k + \Pi^k/\beta))X + \frac{1}{2\eta} \|X - X^k\|_F^2 \\ \text{s.t.} \quad & X^\top X = I. \end{aligned} \quad (8)$$

Denote $M^k = AA^\top X^k + (\alpha(X^k - Y^k + \Lambda^k/\alpha) + \beta(X^k - Z^k + \Pi^k/\beta))$, then problem (8) can be rewritten as

$$\begin{aligned} \min_X \quad & \frac{1}{2\eta} \|X - X^k + \eta M^k\|_F^2 \\ \text{s.t.} \quad & X^\top X = I. \end{aligned} \quad (9)$$

Let $X^k - \eta M^k = U\Sigma V^\top$ be the SVD. Then

$$X^{k+1} = UV^\top, \quad (10)$$

which can be described by the following network

$$X^{k+1} = \text{LargNet}(U, V^\top), \quad (11)$$

where **LargNet** denotes two distinct linear layers, as shown in Fig. 1.

2.2 Update Y^{k+1}

Once X has been updated, Y can be obtained by solving

$$\min_Y \quad \lambda \|Y\|_{2,1} + \frac{\alpha}{2} \|X^{k+1} - Y + \Lambda^k/\alpha\|_F^2. \quad (12)$$

According to the soft thresholding associated with $\ell_{2,1}$ -norm and [29], it has the close-form solution

$$\frac{X^{k+1} + \Lambda^k/\alpha}{\|X^{k+1} + \Lambda^k/\alpha\|_2} \text{ReLU}(\|X^{k+1} + \Lambda^k/\alpha\|_2 - \lambda/\alpha), \quad (13)$$

which can be denoted by the following network

$$Y^{k+1} = \text{GSoftNet}(X^{k+1} + \Lambda^k/\alpha, \lambda/\alpha). \quad (14)$$

We would like to emphasize that this paper uses **GSoftNet** to denote networks involving $\ell_{2,1}$ -norm, and the word **G** comes from group sparsity.

Algorithm 1 SPCA-Net**Input:** Data $A \in \mathbb{R}^{d \times n}$, parameters $\lambda, \mu, \alpha, \beta$ **Initialize:** $(X^0, Y^0, Z^0, \Lambda^0, \Pi^0)$ **While** not converged **do**1: Update X^{k+1} by

$$X^{k+1} = \text{LargNet}(U, V^\top)$$

2: Update Y^{k+1} by

$$Y^{k+1} = \text{GSoftNet}(X^{k+1} + \Lambda^k / \alpha, \lambda / \alpha)$$

3: Update Z^{k+1} by

$$Z^{k+1} = \text{SoftNet}(X^{k+1} + \Pi^k / \beta, \mu / \beta)$$

4: Update Λ^{k+1}, Π^{k+1} by

$$\Lambda^{k+1} = \text{Linear}(\Lambda^k, X^{k+1}, Y^{k+1}, \alpha)$$

$$\Pi^{k+1} = \text{Linear}(\Pi^k, X^{k+1}, Z^{k+1}, \beta)$$

End while**Output:** Trained X **2.3 Update Z^{k+1}** After X, Y have been updated, Z can be solved by

$$\min_Z \mu \|Z\|_1 + \frac{\beta}{2} \|X^{k+1} - Z + \Pi^k / \beta\|_F^2. \quad (15)$$

Similar to the Y -subproblem, invoking the soft thresholding associated with ℓ_1 -norm, it has the close-form solution

$$\frac{X^{k+1} + \Pi^k / \beta}{|X^{k+1} + \Pi^k / \beta|} \text{ReLU}(|X^{k+1} + \Pi^k / \beta| - \mu / \beta), \quad (16)$$

which can be characterized by the following network

$$Z^{k+1} = \text{SoftNet}(X^{k+1} + \Pi^k / \beta, \mu / \beta). \quad (17)$$

Here, **SoftNet** denotes networks that involve ℓ_1 -norm.**2.4 Update Λ^{k+1}, Π^{k+1}**

The Lagrange multipliers can be calculated by

$$\begin{aligned} \Lambda^{k+1} &= \Lambda^k + \alpha(X^{k+1} - Y^{k+1}), \\ \Pi^{k+1} &= \Pi^k + \beta(X^{k+1} - Z^{k+1}), \end{aligned} \quad (18)$$

which can be represented by the following networks

$$\begin{aligned} \Lambda^{k+1} &= \text{Linear}(\Lambda^k, X^{k+1}, Y^{k+1}, \alpha), \\ \Pi^{k+1} &= \text{Linear}(\Pi^k, X^{k+1}, Z^{k+1}, \beta). \end{aligned} \quad (19)$$

In summary, the complete deep unfolding architecture for solving problem (3) is presented in Algorithm 4 and Fig. 1. Our framework eliminates manual parameter tuning through full parameter learnability, encompassing both regularization parameters (λ, μ) and penalty parameters (α, β) . In addition, the loss function is defined as

$$\text{Loss} = \frac{1}{2} \|A - \bar{X} \bar{X}^\top A\|_F^2 + \lambda \|\bar{X}\|_{2,1} + \mu \|\bar{X}\|_1, \quad (20)$$

where \bar{X} represents the predicted matrix.

Table 1: The dataset information.

| Datasets | Features | Samples | Categories | Types |
|----------|----------|---------|------------|-------------|
| COIL20 | 1024 | 1440 | 20 | Image |
| Isolet | 617 | 1560 | 26 | Speech |
| UMIST | 644 | 575 | 20 | Handwritten |
| MSTAR | 1024 | 2425 | 10 | Biological |

3 Experiments

This section demonstrates the superiority of our proposed method for the UFS task on four public datasets; see Table 1 for more details.

3.1 Parameter Setup

In experiments, the compared methods include LapScore [30], UDFS [31], SOGFS [32], RNE [33], FSPCA [34], and SPCAFS [35]. Among them, LapScore, UDFS, SOGFS, and RNE are directly implemented by the AutoUFSTool toolbox¹. SPCAFS can be downloaded from the author's link². For the above methods, the default parameters are adopted. For our proposed SPCA-Net, the number of network layers is set to 5. In addition, all features marked as ALLfea are used as baselines for comparison.

To evaluate the compared methods, two popular metrics, i.e., clustering accuracy (ACC) and normalized mutual information (NMI), are used. As suggested in [35], the number of selected features is chosen from 10 to 100. To ensure fairness and reduce the variations caused by different initial conditions, the k -means clustering algorithm is repeated 50 times. Therefore, the final results are presented as the average and standard deviation of these 50 runs.

3.2 Numerical Results

Fig. 2 and Fig. 3 show the comparative ACC and NMI metrics across feature dimensions, respectively. It can be seen that as the number of selected features increases, the metrics of all compared methods improve to some extent, but in most cases, our proposed SPCA-Net can achieve the best performance. Although our proposed SPCA-Net does not perform particularly well when there are fewer selected features, as the number increases, the performance will improve significantly until it exceeds others.

Further, Table 2 and Table 3 quantify the corresponding ACC and NMI results, respectively. Additionally, their average values and standard deviations are provided, with the best results marked in bold. It can be concluded that for all datasets, our proposed SPCA-Net consistently outperforms the other compared methods. In particular, for the Isolet dataset, the ACC value of SPCA-Net is 59.17%, and the corresponding NMI value is 75.35%, which are 5.02% and 4.20% higher than the second-place method, respectively.

3.3 Ablation Studies

Table 4 lists the clustering results without and with the network, where \times means that the regularization parameters are selected by grid search. It can be seen that deep unfolding networks can significantly improve ACC and NMI. In fact, In fact, it is quite difficult for grid search to find out

¹<https://github.com/farhadabedinzadeh/AutoUFSTool>²<https://github.com/quiter2005/algorithm>

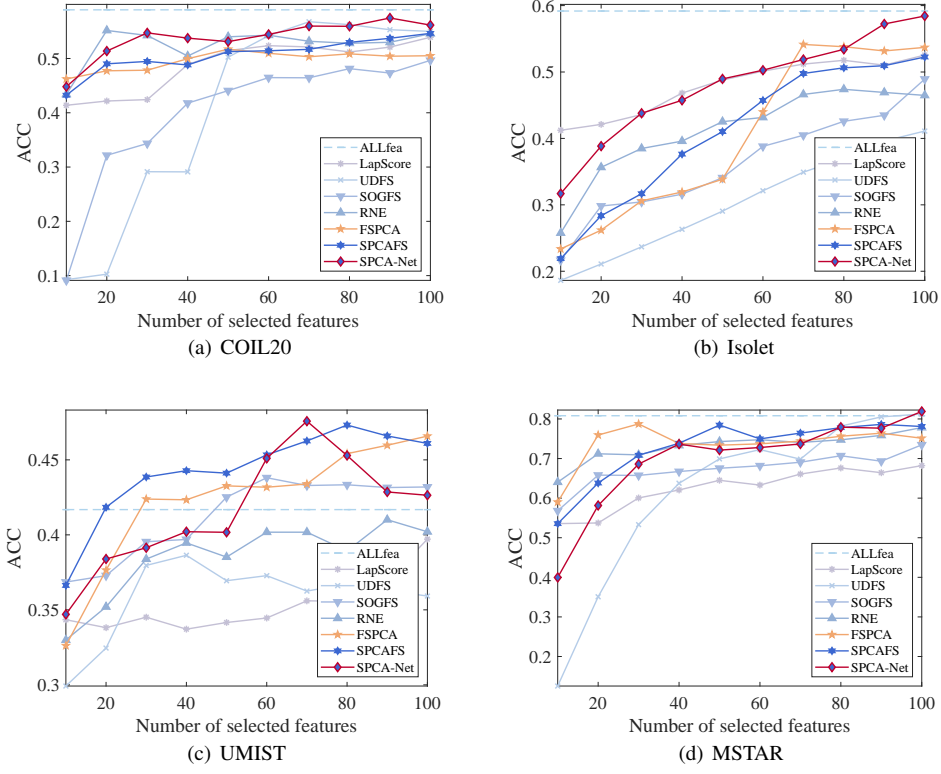


Fig. 2: Visualization of ACC results for all compared methods.

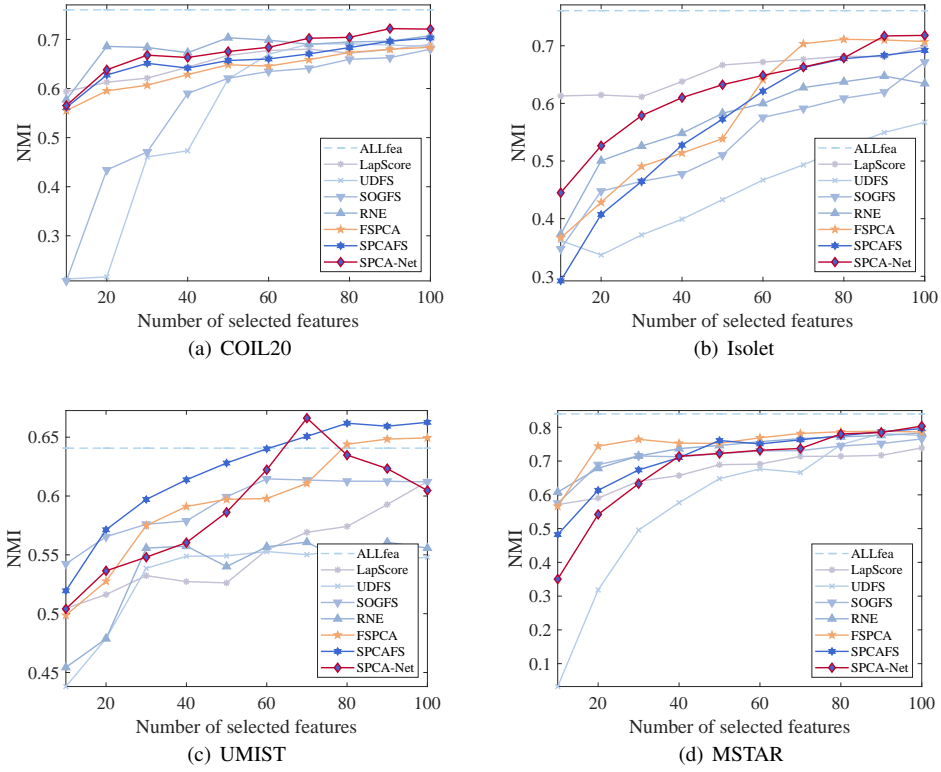


Fig. 3: Visualization of NMI results for all compared methods.

the proper regularization parameters. In addition, Table 5 lists the clustering results without and with dynamic parameters, where \times indicates that the regularization parameters

are fixed during the network iterations. Obviously, the dynamic parameters can better adapt to the data. The above ablation experiments validate the necessity of our method.

Table 2: ACC results (mean % \pm std %) for all compared methods.

| Datasets | ALLfea | LapScore [30] | UDFS [31] | SOGFS [32] | RNE [33] | FSPCA [34] | SPCAFS [35] | SPCA-Net |
|----------|--------------------------|---------------------------|---------------------------|---------------------------|---------------------------|---------------------------|---------------------------|--|
| COIL20 | 58.97 \pm 4.99 (10) | 53.91 \pm 3.61 (100) | 56.70 \pm 3.09 (70) | 49.66 \pm 3.63 (100) | 55.16 \pm 3.35 (20) | 51.71 \pm 3.05 (50) | 54.63 \pm 3.64 (100) | 57.46\pm2.76 (90) |
| Isolet | 59.18 \pm 3.19 (10) | 52.55 \pm 2.83 (100) | 41.11 \pm 1.71 (100) | 48.93 \pm 2.69 (100) | 47.39 \pm 2.91 (80) | 54.15 \pm 2.69 (70) | 52.26 \pm 2.81 (100) | 58.43\pm4.31 (100) |
| UMIST | 41.68 \pm 2.46 (10) | 39.71 \pm 3.28 (100) | 38.64 \pm 1.61 (40) | 43.81 \pm 2.98 (80) | 41.01 \pm 2.25 (90) | 46.58 \pm 2.34 (100) | 47.32 \pm 3.48 (80) | 47.58\pm4.97 (70) |
| MSTAR | 80.81 \pm 8.76 (10) | 68.21 \pm 4.57 (100) | 81.25 \pm 7.48 (100) | 73.46 \pm 5.61 (100) | 77.82 \pm 6.16 (100) | 78.74 \pm 5.20 (30) | 78.63 \pm 8.68 (90) | 81.90\pm6.87 (100) |

Table 3: NMI results (mean % \pm std %) for all compared methods.

| Datasets | ALLfea | LapScore [30] | UDFS [31] | SOGFS [32] | RNE [33] | FSPCA [34] | SPCAFS [35] | SPCA-Net |
|----------|--------------------------|---------------------------|---------------------------|---------------------------|---------------------------|---------------------------|---------------------------|--|
| COIL20 | 76.04 \pm 1.69 (10) | 69.01 \pm 1.53 (100) | 69.12 \pm 1.17 (80) | 68.03 \pm 1.59 (100) | 70.76 \pm 2.07 (100) | 68.41 \pm 1.60 (100) | 70.29 \pm 1.31 (100) | 72.21\pm2.68 (90) |
| Isolet | 76.09 \pm 1.77 (10) | 69.86 \pm 1.26 (100) | 56.73 \pm 1.05 (100) | 67.15 \pm 1.45 (100) | 64.74 \pm 1.28 (90) | 71.12 \pm 1.11 (80) | 69.18 \pm 1.33 (100) | 71.80\pm1.59 (100) |
| UMIST | 64.07 \pm 1.76 (10) | 61.23 \pm 2.15 (100) | 55.43 \pm 1.50 (80) | 61.46 \pm 2.03 (70) | 56.08 \pm 1.80 (60) | 64.94 \pm 1.65 (100) | 66.26 \pm 1.74 (100) | 66.62\pm7.52 (70) |
| MSTAR | 83.96 \pm 3.14 (10) | 73.90 \pm 1.62 (100) | 78.18 \pm 3.64 (90) | 76.56 \pm 1.54 (100) | 78.26 \pm 2.51 (100) | 78.87 \pm 2.52 (90) | 79.62 \pm 2.30 (100) | 80.67\pm3.47 (90) |

Table 4: Ablation studies for the network.

| Datasets | Network | ACC | NMI |
|----------|--------------|----------------------------------|----------------------------------|
| COIL20 | \times | 55.12 \pm 2.67 | 70.44 \pm 1.37 |
| | \checkmark | 57.46\pm2.76 | 72.21\pm2.68 |
| Isolet | \times | 51.84 \pm 2.82 | 67.02 \pm 1.43 |
| | \checkmark | 58.43\pm4.31 | 71.80\pm1.59 |
| UMIST | \times | 40.65 \pm 2.29 | 55.88 \pm 1.62 |
| | \checkmark | 47.58\pm4.97 | 66.62\pm7.52 |
| MSTAR | \times | 80.65 \pm 6.47 | 80.53 \pm 2.41 |
| | \checkmark | 81.90\pm6.87 | 80.67\pm3.47 |

Table 5: Ablation studies for dynamic parameters.

| Datasets | Dynamic | ACC | NMI |
|----------|--------------|----------------------------------|----------------------------------|
| COIL20 | \times | 56.71 \pm 3.83 | 71.49 \pm 3.67 |
| | \checkmark | 57.46\pm2.76 | 72.21\pm2.68 |
| Isolet | \times | 52.06 \pm 3.71 | 68.91 \pm 2.36 |
| | \checkmark | 58.43\pm4.31 | 71.80\pm1.59 |
| UMIST | \times | 42.63 \pm 2.78 | 60.12 \pm 1.69 |
| | \checkmark | 47.58\pm4.97 | 66.62\pm7.52 |
| MSTAR | \times | 80.74 \pm 5.28 | 80.59 \pm 3.67 |
| | \checkmark | 81.90\pm6.87 | 80.67\pm3.47 |

3.4 Remark

Compared with traditional numerical optimization, which often requires hundreds or thousands of iterations, deep unfolding networks only require less than 10 stages to achieve good results; see Fig. 4. However, it should be noted that the performance will degrade if the number of iterations exceeds a certain number, so in practice we chose between 3 and 5.

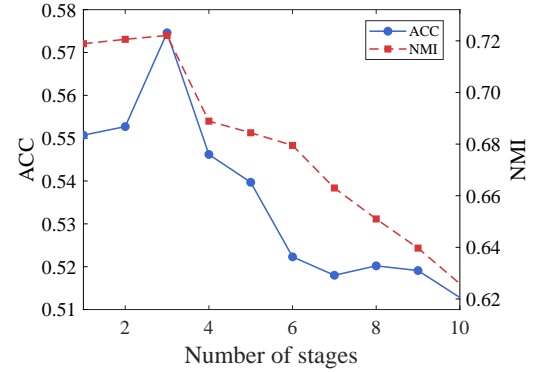


Fig. 4: Visualization of deep unfolding stages on COIL20.

4 Conclusion

In this paper, we mathematically construct a structured sparse PCA model and combine it with deep unfolding networks to propose an encouraging UFS approach. It can not only learn the regularization parameters of the model, but also learn the penalty parameters in ADMM, thus providing a tuning-free algorithm. To the best of our knowledge, this is the first time that attempts to investigate deep unfolding networks for UFS. Experimental results demonstrate that even compared with the state-of-the-art FSPCA and SPCAFS, the proposed method still delivers superior performance in terms of ACC and NMI.

In the future we are interested in designing more effective loss functions and extending it to deep equilibrium networks [36] to further improve the performance.

References

- [1] J. Li, K. Cheng, S. Wang, F. Morstatter, R. P. Trevino, J. Tang, and H. Liu, "Feature selection: A data perspective," *ACM Computing Surveys*, vol. 50, no. 6, pp. 1–45, 2017.
- [2] S. Solorio-Fernández, J. A. Carrasco-Ochoa, and J. F. Martínez-Trinidad, "A review of unsupervised feature selection methods," *Artificial Intelligence Review*, vol. 53, no. 2, pp. 907–948, 2020.
- [3] G. Li, Z. Yu, K. Yang, M. Lin, and C. P. Chen, "Exploring feature selection with limited labels: A comprehensive survey of semi-supervised and unsupervised approaches," *IEEE Transactions on Knowledge and Data Engineering*, vol. 36, no. 11, pp. 6124–6144, 2024.
- [4] H. Zou and L. Xue, "A selective overview of sparse principal component analysis," *Proceedings of the IEEE*, vol. 106, no. 8, pp. 1311–1320, 2018.
- [5] A. M. Rekaivandi, A.-K. Seghouane, and R. J. Evans, "Learning robust and sparse principal components with the α -divergence," *IEEE Transactions on Image Processing*, vol. 33, pp. 3441–3455, 2024.
- [6] Q. Zhou, Q. Wang, Q. Gao, M. Yang, and X. Gao, "Unsupervised discriminative feature selection via contrastive graph learning," *IEEE Transactions on Image Processing*, vol. 33, pp. 972–986, 2024.
- [7] X. Xiu, Y. Yang, L. Kong, and W. Liu, "Laplacian regularized robust principal component analysis for process monitoring," *Journal of Process Control*, vol. 92, pp. 212–219, 2020.
- [8] X. Xiu, Z. Miao, and W. Liu, "A sparsity-aware fault diagnosis framework focusing on accurate isolation," *IEEE Transactions on Industrial Informatics*, vol. 19, no. 2, pp. 1356–1365, 2023.
- [9] R. Drikvandi and O. Lawal, "Sparse principal component analysis for natural language processing," *Annals of Data Science*, vol. 10, no. 1, pp. 25–41, 2023.
- [10] M. S. Jahan and M. Oussalah, "A systematic review of hate speech automatic detection using natural language processing," *Neurocomputing*, vol. 546, p. 126232, 2023.
- [11] H. Zou, T. Hastie, and R. Tibshirani, "Sparse principal component analysis," *Journal of Computational and Graphical Statistics*, vol. 15, no. 2, pp. 265–286, 2006.
- [12] X. Xiu, Y. Yang, L. Kong, and W. Liu, "Data-driven process monitoring using structured joint sparse canonical correlation analysis," *IEEE Transactions on Circuits and Systems II: Express Briefs*, vol. 68, no. 1, pp. 361–365, 2021.
- [13] J. Liu, S. Ji, and J. Ye, "Multi-task feature learning via efficient $\ell_{2,1}$ -norm minimization," in *Proceedings of the Twenty-Fifth Conference on Uncertainty in Artificial Intelligence*, pp. 339–348, 2009.
- [14] F. Nie, H. Huang, X. Cai, and C. Ding, "Efficient and robust feature selection via joint $\ell_{2,1}$ -norms minimization," *Advances in Neural Information Processing Systems*, vol. 23, 2010.
- [15] J. Snoek, H. Larochelle, and R. P. Adams, "Practical Bayesian optimization of machine learning algorithms," *Advances in Neural Information Processing Systems*, vol. 25, 2012.
- [16] P. Shang and L. Kong, " ℓ_1 -norm quantile regression screening rule via the dual circumscribed sphere," *IEEE Transactions on Pattern Analysis and Machine Intelligence*, vol. 44, no. 10, pp. 6254–6263, 2022.
- [17] Y. Tian and Y. Zhang, "A comprehensive survey on regularization strategies in machine learning," *Information Fusion*, vol. 80, pp. 146–166, 2022.
- [18] K. Gregor and Y. LeCun, "Learning fast approximations of sparse coding," in *Proceedings of the 27th International Conference on Machine Learning*, pp. 399–406, 2010.
- [19] V. Monga, Y. Li, and Y. C. Eldar, "Algorithm unrolling: Interpretable, efficient deep learning for signal and image processing," *IEEE Signal Processing Magazine*, vol. 38, no. 2, pp. 18–44, 2021.
- [20] J. Zhang, B. Chen, R. Xiong, and Y. Zhang, "Physics-inspired compressive sensing: Beyond deep unrolling," *IEEE Signal Processing Magazine*, vol. 40, no. 1, pp. 58–72, 2023.
- [21] N. Shlezinger, J. Whang, Y. C. Eldar, and A. G. Dimakis, "Model-based deep learning," *Proceedings of the IEEE*, vol. 111, no. 5, pp. 465–499, 2023.
- [22] N. T. Nguyen, L. V. Nguyen, N. Shlezinger, Y. C. Eldar, A. L. Swindlehurst, and M. Juntti, "Joint communications and sensing hybrid beamforming design via deep unfolding," *IEEE Journal of Selected Topics in Signal Processing*, vol. 18, no. 5, pp. 901–916, 2024.
- [23] Y. Yang, J. Sun, H. Li, and Z. Xu, "ADMM-CSNet: A deep learning approach for image compressive sensing," *IEEE Transactions on Pattern Analysis and Machine Intelligence*, vol. 42, no. 3, pp. 521–538, 2020.
- [24] F. Wu, T. Zhang, L. Li, Y. Huang, and Z. Peng, "RPCANet: Deep unfolding RPCA based infrared small target detection," in *Proceedings of the IEEE/CVF Winter Conference on Applications of Computer Vision*, pp. 4809–4818, 2024.
- [25] S. Mukherjee, A. Hauptmann, O. Öktem, M. Pereyra, and C.-B. Schönlieb, "Learned reconstruction methods with convergence guarantees: A survey of concepts and applications," *IEEE Signal Processing Magazine*, vol. 40, no. 1, pp. 164–182, 2023.
- [26] X. Chen, J. Liu, and W. Yin, "Learning to optimize: A tutorial for continuous and mixed-integer optimization," *Science China Mathematics*, vol. 67, no. 6, pp. 1191–1262, 2024.
- [27] N. Simon, J. Friedman, T. Hastie, and R. Tibshirani, "A sparse-group lasso," *Journal of Computational and Graphical Statistics*, vol. 22, no. 2, pp. 231–245, 2013.
- [28] D.-R. Han, "A survey on some recent developments of alternating direction method of multipliers," *Journal of the Operations Research Society of China*, pp. 1–52, 2022.
- [29] C. Li, B. Zhang, D. Hong, J. Yao, and J. Chanussot, "LRR-Net: An interpretable deep unfolding network for hyperspectral anomaly detection," *IEEE Transactions on Geoscience and Remote Sensing*, vol. 61, pp. 1–12, 2023.
- [30] X. He, D. Cai, and P. Niyogi, "Laplacian score for feature selection," *Advances in Neural Information Processing Systems*, vol. 18, 2005.
- [31] Y. Yang, H. T. Shen, Z. Ma, Z. Huang, and X. Zhou, " $\ell_{2,1}$ -norm regularized discriminative feature selection for unsupervised learning," in *IJCAI International Joint Conference on Artificial Intelligence*, 2011.
- [32] F. Nie, W. Zhu, and X. Li, "Unsupervised feature selection with structured graph optimization," in *Proceedings of the AAAI Conference on Artificial Intelligence*, vol. 30, 2016.
- [33] Y. Liu, D. Ye, W. Li, H. Wang, and Y. Gao, "Robust neighborhood embedding for unsupervised feature selection," *Knowledge-Based Systems*, vol. 193, p. 105462, 2020.
- [34] F. Nie, L. Tian, R. Wang, and X. Li, "Learning feature-sparse principal subspace," *IEEE Transactions on Pattern Analysis and Machine Intelligence*, vol. 45, no. 4, pp. 4858–4869, 2023.
- [35] Z. Li, F. Nie, J. Bian, D. Wu, and X. Li, "Sparse PCA via $\ell_{2,p}$ -norm regularization for unsupervised feature selection," *IEEE Transactions on Pattern Analysis and Machine Intelligence*, vol. 45, no. 4, pp. 5322–5328, 2023.
- [36] D. Gilton, G. Ongie, and R. Willett, "Deep equilibrium architectures for inverse problems in imaging," *IEEE Transactions on Computational Imaging*, vol. 7, pp. 1123–1133, 2021.